Hydrol. Earth Syst. Sci. Discuss., 12, 2201–2242, 2015
www.hydrol-earth-syst-sci-discuss.net/12/2201/2015/
doi:10.5194/hessd-12-2201-2015
© Author(s) 2015. CC Attribution 3.0 License.

Hydrology and Earth System Sciences
Discussions
Open Access

This discussion paper is/has been under review for the journal Hydrology and Earth System Sciences (HESS). Please refer to the corresponding final paper in HESS if available.

Isolating the impacts of land use and climate change on streamflow

I. Chawla[1] **and P. P. Mujumdar**[1,2]

[1]Department of Civil Engineering, Indian Institute of Science, Bangalore, India
[2]Divecha Center for Climate Change, Indian Institute of Science, Bangalore, India

Received: 26 January 2015 – Accepted: 2 February 2015 – Published: 20 February 2015

Correspondence to: P. P. Mujumdar (pradeep@civil.iisc.ernet.in)

Published by Copernicus Publications on behalf of the European Geosciences Union.

Isolating the impacts of land use and climate change on streamflow

I. Chawla and P. P. Mujumdar

CC BY

Abstract

Streamflow regime is sensitive to changes in land use and climate in a river basin. Quantifying the isolated and integrated impacts of land use and climate change on streamflow is challenging as well as crucial to optimally manage water resources in the river basin. This paper presents a simple hydrologic modelling based approach to segregate the impacts of land use and climate change on streamflow of a river basin. The upper Ganga basin in India is selected as the case study to carry out the analysis. Streamflow in the river basin is modelled using a calibrated variable infiltration capacity hydrologic model. The approach involves development of three scenarios to understand the influence of land use and climate on streamflow. The first scenario assesses the sensitivity of streamflow to land use changes under invariant climate. The second scenario determines the change in streamflow due to change in climate assuming constant land use. The third scenario estimates the combined effect of changing land use and climate over streamflow of the basin. Based on the results obtained from the three scenarios, quantification of isolated impacts of land use and climate change on streamflow is addressed. Future projections of climate are obtained from dynamically downscaled simulations of six general circulation models (GCMs) available from the Coordinated Regional Downscaling Experiment (CORDEX) project. Uncertainties associated with the GCMs and emission scenarios are quantified in the analysis. Results for the case study indicate that streamflow is highly sensitive to change in urban area and moderately sensitive to change in crop land area. However, variations in streamflow generally reproduce the variations in precipitation. Combined effect of land use and climate on streamflow is observed to be more pronounced compared to their individual impacts in the basin. It is observed from the isolated effects of land use and climate change that climate has a more dominant impact on streamflow in the region. The approach proposed in this paper is applicable to any river basin to isolate the impacts of land use change and climate change on the streamflow.

HESSD

12, 2201–2242, 2015

Isolating the impacts of land use and climate change on streamflow

I. Chawla and P. P. Mujumdar

CC BY

1 Introduction

Land use (LU) and climate are the drivers of hydrologic processes in a river basin (Vörösmarty, 2000; Nijssen et al., 2001; Oki and Kanae, 2006; Wada et al., 2011). Change in LU is observed to influence the hydrological cycle and the availability of water resources by altering interception, infiltration rate, albedo and evapotranspiration (ET) (Rose and Peters, 2001; Scanlon et al., 2007; Rientjes et al., 2011). Climate in contrast affects the basic components of hydrologic cycle such as precipitation, soil moisture, evaporation and atmospheric water content (Wang et al., 2008). With increase in scarcity of water resources, hydrologic impacts of LU and climate change has drawn significant attention from the hydrologic community (Scanlon et al., 2007). In this regard, several studies have been carried out that focus on understanding exclusive impacts of either of the two drivers (Hamlet and Lettenmaier, 1999; Christensen and Lettenmaier, 2007; Beyene et al., 2010; Wagner et al., 2013; Islam et al., 2014). Optimum management of water resources in a river basin needs an in depth understanding of the isolated and integrated effects of LU and climate on streamflow. Due to nonlinear and complicated response of streamflow to combined effects of LU and climate change (Fu et al., 2007), very few studies have been carried out on this aspect (Mango et al., 2011; Cuo et al., 2013). Segregating the individual contribution of LU and climate to streamflow has recently become the focus of scientific work (Wang and Hejazi, 2011; Wang et al., 2013; Renner et al., 2012, 2014). This paper presents a simple hydrologic modelling based approach to isolate the impacts of land use and climate on streamflow. The analysis is carried out on Ganga river basin since there is dearth of studies that comprehensively examine the effects of LU and climate change on streamflow in this basin.

Originating from the Himalayas, the river Ganga traverses a stretch of 2525 km covering a catchment area of around 800 000 km^2 which is approximately 26 % of the entire India's land mass making it the largest river basin in India. During its course, Ganga flows through some of the major states of India harboring about 44 % of coun-

HESSD
12, 2201–2242, 2015

CC BY

try's population (http://censusindia.gov.in/). Due to presence of alluvium, the basin is very fertile and forms close to 30 % of India's cultivable area (http://eands.dacnet.nic.in/LUS_2001-11.htm). Thus there is a clear consensus that the river is of great social and economic importance to India. In this study, the area under investigation is the upstream reaches of the Ganga basin encompassing river's originating place (Fig. 1). This region is referred as the Upper Ganga Basin (UGB) in the paper.

Methods used to assess the impacts of LU and climate on streamflow can be broadly classified into four categories (i) experimental paired catchment approach, (ii) statistical techniques such as Mann–Kendall test, (iii) empirical or conceptual models and (iv) distributed physically-based hydrologic models. The first three approaches may not be suitable for conducting impact assessment studies since they are either extremely data intensive (to be applicable over large catchments) or lack physical mechanisms (to attribute the observed changes to appropriate causes). Therefore, one is left with the option of using distributed physically based hydrologic models, which are by far the most appealing tools to carry out impact assessment studies (Ott and Uhlenbrook, 2004; Mango et al., 2011; Wang et al., 2012). These models operate within a distributed framework to take physical and meteorological conditions of the basin into account (Refsgaard and Knudsen, 1996). In this study, the physically-based macroscale Variable Infiltration Capacity (VIC) hydrologic model (Liang et al., 1994) has been employed for the analysis.

In order to obtain the isolated impacts of LU and climate change on streamflow, following objectives are addressed in the current work: (i) assess sensitivity of the streamflow to changes in different LU categories, (ii) examine impacts of climate change on the streamflow and (iii) analyze integrated impacts of LU and climate change on the streamflow. The three objectives are translated into three scenarios wherein first two scenarios quantify the independent effects of LU and climate on streamflow under their invariant counterparts i.e., climate and LU respectively are kept constant. The third scenario deals with concurrent changes in LU and climate. Results from the three scenarios are further used to segregate the hydrologic impacts of LU and climate change. The

HESSD
12, 2201–2242, 2015

aforementioned objectives are investigated over the UGB as a case study by employing a calibrated and validated VIC model to simulate streamflows. To assess the impact of future climate on streamflow in the basin, dynamically downscaled climate simulations for six GCMs obtained from the CORDEX project are used. Climate change related analyses are carried out under the uncertainty framework to address two issues, one, climate models based uncertainties, and two, emission scenarios based uncertainties.

2 Data and methods

2.1 Study area

The UGB, located within geographic coordinates of 25°30′ to 31°30′ N latitude and 77°30′ to 80° E longitudes (Fig. 1), drains a catchment area of 95 593 km^2. While most of the Ganga basin comprises of agricultural areas with reasonably flat terrain, this region (UGB) is the only part of the Ganga basin which is characterized by wide variation in topography with elevations ranging from 21 to 7796 m (Fig. 1), thus making it an interesting case study for investigation. In addition, since the river Ganga originates in this region, any change in hydrologic response due to LU and/or climate is likely to affect the entire flow regime downstream. Thus this region is critical for assessing the impact of LU and climate change on the streamflow of the basin. In the backdrop of recent flood event in July 2013 in the UGB, which has been attributed to climate change (Singh et al., 2014), isolating the hydrologic impacts of changing LU and climate in this basin has become much more important.

In this study, the UGB is divided into three regions, upstream, midstream and downstream (Fig. 1) based on altitude, topography and land use characteristics. The upstream region is highly mountainous, characterized by glaciers and dense forests having elevations from 297 to 7796 m. From upstream to midstream region, there is transition from hills to plains. Midstream region is dominated by forests and crop lands with elevations ranging from 75 to 3079 m. The downstream region is mostly covered

HESSD
12, 2201–2242, 2015

by crop lands having consistent elevations of around 100 m. In addition to the varying land use characteristics, these three regions have different climatology as well. From 1971 to 2005, upstream, midstream and downstream regions recorded an average annual precipitation of 1294, 1009 and 826 mm respectively. Most of the precipitation is concentrated during the monsoon months from June to September (JJAS). Average annual temperatures across the three regions during the same period were 20, 23 and 26 °C respectively. Due to significant variation in the characteristics of these regions, they are modelled separately in the paper. Details of data required to drive the hydrologic model are presented in the following section.

2.2 Input data for the hydrologic model

The current study requires topographic, soil, hydro-meteorological and LU data which are procured from various sources. Topographic information is obtained from ASTER (Advanced Spaceborne Thermal Emission and Reflection Radiometer) DEM (Digital Elevation Model) available at 30 m spatial resolution. Digital soil map for the region is procured from National Bureau of Soil Survey and Land Use Planning, India at a scale of 1 : 250 000. Meteorological data (rainfall, maximum temperature, minimum temperature and wind speed) for the period 1971–2005 at daily time scale is procured from two sources: Indian Meteorological Department (IMD) (Rajeevan et al., 2006) and Princeton University (PU) (Sheffield et al., 2006). Meteorological data from both the sources are brought to a common grid resolution of 0.5° which also serves as the resolution for executing the VIC hydrologic model. Observed streamflow data (Q_{obs}) for two locations: Bhimgodha (1987–2011) and Ankinghat (1977–2009) is obtained (at monthly scale) from Uttar Pradesh Irrigation Department and Central Water Commission. Along with Q_{obs}, data corresponding to various diversion channels is also procured to convert the observed (regulated) flow to natural flow. The flow data thus obtained ($Q_{n-\text{obs}}$) is used for model calibration and validation.

For LU data, landsat imageries for the years 1973, 1980, 2000 and 2011 are selected and then classified to determine the LU change in the basin over four decades. Field

HESSD
12, 2201–2242, 2015

study is carried out to collect the training sites for image classification. The accuracy of classified images is obtained to be 89, 83, 88 and 79 % for 1973, 1980, 2000 and 2011 images respectively which is seen to be generally good. Thus the classified images can be used as LU maps of the UGB for the corresponding time periods. Results of classification and change in LU are presented in Sect. 3.1.

To carry out hydrologic impact studies related to climate change, one needs data on future climate variables such as rainfall (P), temperature (T) and wind speed (W) which in the current study is procured from CORDEX South Asia group (http://cccr.tropmet.res.in/cordex/index.jsp) at daily scale for six Coupled Model Intercomparison Project 5 (CMIP5) GCM simulations (Table 1). Each model has a time series for all the requisite variables corresponding to the twentieth century climate (historic run) and future climate using Representative Concentration Pathway, RCP 4.5 and RCP 8.5 emission scenarios. All the GCM outputs are brought to a consistent resolution of 0.5°.

It is now well known that large scale pattern of climate variables simulated by GCMs may be realistic, but when downscaled to regional level, they may exhibit significant bias compared to the observed data (Maurer and Hidalgo, 2008; Ghosh and Mujumdar, 2009). This can have significant effect on hydrological impact studies which necessitates the need of performing bias correction on the climate variables obtained. In the current work P, T and W generated from GCMs are bias corrected with IMD gridded data (which is considered as observed data) using the technique developed by Wood et al., (2002).

Statistics of GCM simulated (post bias correction) and observed climate variables for upstream region are presented in Taylor diagram (Fig. 2). It can be observed that all the models are clustered together which could be due to the fact that all the GCM outputs are from the same modelling center and, the clusters in case of T_{max} (maximum temperature) and T_{min} (minimum temperature) (Fig. 2b and c respectively) are closer to the observed data (represented by point 'a') which reflects a better quality of GCM outputs for T. In case of P (Fig. 2a), it is observed that the models' cluster is slightly far from point 'a', nevertheless, reasonably good correlation of 0.6–0.7 exists between GCM P

HESSD
12, 2201–2242, 2015

CC BY

and observed P. Similar inferences are drawn from the analyses over midstream and downstream regions. Based on the statistics obtained, downscaled variables are considered to reasonably represent the climate of the region and are further used to drive the VIC model.

2.3 VIC hydrologic model: description, calibration and validation

The VIC model is a semi-distributed soil-vegetation-atmosphere-transfer model that solves coupled water and energy balance equations grid wise to calculate different hydrologic components (Liang et al., 1994). Within a grid the VIC model considers subgrid heterogeneity by dividing each grid cell into number of tiles which in turn depend on different land use types present in the grid. Each tile generates different response to the precipitation in the form of infiltration, soil moisture storage, runoff and evaporation, owing to difference in land surface properties. When VIC concludes the computation of energy and water balance calculations for each grid within the watershed, streamflow routing model developed by Lohmann et al. (1998) is activated that transports the surface runoff generated within a grid along with the baseflow to the outlet of grid cell which is further routed through the river channel to the watershed outlet.

For the model calibration in the present work, three parameters as suggested by Lohmann et al. (1998) are calibrated to obtain an optimum combination such that the error between observed and simulated streamflow is minimum. The three parameters considered are (i) B – variable infiltration curve parameter, (ii) Ds – fraction of maximum velocity of baseflow where nonlinear baseflow begins, and (iii) Ws – fraction of maximum soil moisture where nonlinear baseflow occurs. According to Liang et al. (1994) the parameter B has largest effect on runoff hydrograph and Ds and Ws parameters are critical in influencing the baseflow. Calibration of these parameters is necessary since their values vary with watersheds. Moreover, these are the only three parameters which are unknown in the present study. All the other parameters (http://www.hydro.washington.edu/Lettenmaier/Models/VIC/Documentation/SoilParam.shtml) are obtained from the soil map used in this study.

HESSD
12, 2201–2242, 2015

cc BY

VIC model is established independently for upstream, midstream and downstream regions but model calibration became possible only for upstream and midstream regions since Q_{obs} is not available for the downstream region. To address this issue, utilizing the facts that the downstream region has soil type similar to that of midstream region (loam and sandy loam) and the three parameters are essentially influenced by soil, it is assumed that the calibrated parameters obtained for midstream will hold good for downstream region.

To perform model calibration, initially the sensitivity of the simulated discharge to each of the three parameters is tested and their rough estimate of range for both upstream and midstream regions are obtained. Within this range, several candidate models for upstream and midstream regions are created based on several plausible combinations of these three parameters. The VIC model is executed for all the combinations and the one that has maximum predictive power in terms of coefficient of determination (R^2), normalized root mean square error (E_{NRMSE}), nash sutcliffe efficiency (E_{NSE}) and bias (β) for monthly series of simulated streamflow (Q_{sim}) during calibration period is considered. Here, a negative value of β indicates that model overestimates the simulated data and vice versa. It is to be noted that, though the VIC model is executed at daily scale, daily Q_{sim} values are aggregated to monthly values to carry out comparison between Q_{sim} and Q_{n-obs} since Q_{n-obs} is available only at monthly scale.

For the current work, periods of 1987–1999 and 1977–1995 in the upstream and midstream regions respectively are considered for calibration. Figure 3 provides the plots of corresponding observed and calibrated VIC simulated monthly streamflow series for the two regions. It can be observed from Fig. 3 that simulations during the calibration period captured the observed pattern and magnitude of hydrograph very well. In particular, rising and recession limbs of hydrographs are simulated accurately for both the regions. Shortcomings in the VIC simulations for both the regions include mismatch of peak flows which could be due to errors in modelling extreme precipitation by the model. Since we are not dealing with extremes in the present case study, this error is not of much concern. In addition, it may also be observed that at the end of each re-

HESSD
12, 2201–2242, 2015

CC BY

cession limb, there is a sharp drop, which is below the level of $Q_{n-\mathrm{obs}}$. It could be due to inconsideration of baseflow contribution from the ground water in Q_{sim} which needs to be included in Indian watersheds, wherein groundwater serves as major contributor to the streamflow in the form of baseflow during the months of November to March. Also, in the upstream region, some infrequent peaks are simulated by the model during low flow periods which can be attributed to the overestimation of snow melt runoff by the snow module (which is kept active) in the region. Pre and post monsoon rainfall events could also result in this kind of behavior.

The calibrated models are validated from 2000–2005 and from 1996–2005 for the upstream and midstream regions respectively (presented in Fig. 4). Streamflow pattern and magnitude of runoff are well simulated during validation. Table 2 presents optimum set of parameters for the two regions along with their performance measures during calibration and validation. Based on the performance measures it is seen that model is able to predict $Q_{n-\mathrm{obs}}$ reasonably well. Slight negative β (which are evident from scatter plot of Fig. 3a) is observed for upstream region which could be due to overestimation of low flow values. Positive β for midstream region could be due to lack of groundwater contribution to Q_{sim}. The rigorously calibrated and validated VIC model is used to simulate the streamflow under different scenarios considered in the present study.

2.4 GCM and emission scenario uncertainty

Despite strong correlation between the model simulated and observed climate variables (Fig. 2), it is noticed that the magnitude of uncertainty across different models is quite large with respect to observed P and T at annual scale. These uncertainties may get manifested in the hydrologic response (Arnell, 2011) when the future projections are used to drive the VIC hydrologic model for impact assessment. As a result it is essential to quantify the uncertainties associated with both climate data and streamflow generated from the VIC model, which, in the present work, is carried out over six GCMs and two emission scenarios. The uncertainty is quantified with Root Mean

HESSD
12, 2201–2242, 2015

cc BY

Square Difference (σ) metric given by Eq. (1) (Giorgi and Mearns, 2002; Ekström et al., 2007).

$$\sigma = \left[\frac{1}{n}\sum_{i=1}^{n}(\Delta X_i - \overline{\Delta X})^2\right]^{\frac{1}{2}} \tag{1}$$

where, n is the number of GCMs for a given RCP; X is variable under study; ΔX_i is the change in the ith model mean value from the mean of the baseline period of the variable X; $\overline{\Delta X}$ is the ensemble average of change in mean given by Eq. (2)

$$\overline{\Delta X} = \frac{1}{n}\sum_{i=1}^{n}\Delta X_i \tag{2}$$

In the present work, $\overline{\Delta X}$ is considered as estimate of effect of climate change. σ quantifies the average deviation of change in individual model mean from ensemble average of change in mean. Higher the σ, more is the uncertainty associated with the $\overline{\Delta X}$ and consequently less reliable are the results. Further, the ensemble mean of models is statistically analyzed with baseline period's mean to test for equality of means using two sampled t test. The results of t test are interpreted in terms of confidence levels for the change in future projections with respect to baseline period.

In order to infer the confidence level in terms of climatology, classification considered by Maurer (2007) is used according to which, confidence level (i) > 90 % indicates a highly significant change, (ii) 67–90 % indicates moderately significant change, and (iii) < 67 % indicates insignificant change. Furthermore, same test is used to estimate the confidence level with which it can be claimed that the two emission scenarios give statistically different ensemble means. Figure 5 presents the overview of the work.

HESSD
12, 2201–2242, 2015

CC BY

3 Results and discussion

Sections 3.1 and 3.2 provide analysis pertaining to the quantification of changes observed in LU and climate. In Sect. 3.3, these results are used to quantify streamflow variations within the uncertainty framework.

3.1 Analysis of land use

Classification of landsat imageries resulted in LU maps for the UGB which are presented in Fig. 6. It can be observed that the UGB exhibits wide variations in the LU wherein upstream parts are snow covered and downstream parts are crop land. The dominant LU type in the UGB is crop land which covers about 56 % of the entire basin (45, 53, 64 and 66 % for 1973, 1980, 2000 and 2011 respectively). Upon visual examination of figures, it is evident that from 1973 to 2011, area under forest in the upstream region has diminished significantly. Area under different LU categories in the UGB for different time periods is provided in Table 3.

It should be noted that for the present study, detailed snow cover mapping is not performed. Thus the area observed under snow category in Table 3 should not be considered as a trend in the snow cover of the region. Change in area observed for urban land appears to be very high, but spatially it occupies very less area in the entire basin. There has been a decline in dense forest area from 1973 to 2000 followed by an increase. The reason could be attributed to better forest management strategies that are introduced in the region after creation of Uttarakhand state in November 2000. It is observed that there is slight increase in surface area of water which could be attributed to development of structures such as Ramganga reservoir (Fig. 1) after 1973. Results reflect that there has been a massive increase in the area under cultivation in the basin. The dynamics of LU is heavily supported by rapid increase in population of the region (120 % increase between 2001 and 2011 as per census of India, http://censusindia.gov.in/). The impact of changes in LU over streamflow is assessed in Sect. 3.3.1. The following section provides analysis of climate change in the UGB.

HESSD
12, 2201–2242, 2015

CC BY

3.2 Analysis of general circulation model outputs

The projections of rainfall (P) obtained from GCMs are preliminarily examined for long term trends using Mann–Kendall test (Mann, 1945; Kendall, 1938). It is observed that the annual P exhibits a monotonic increase for upstream, midstream and downstream regions with large inter annual variability. In order to determine the change in the climatology of the three regions, outputs from GCMs for future time period are aggregated into five time slices T1 (2010–2020), T2 (2021–2040), T3 (2041–2060), T4 (2061–2080) and T5 (2081–2100). Further on, comparisons are made between the means of the future time slices' and the baseline period (1971–2005). Figure 7 (top panel) shows average change in annual P over all GCMs ("ensemble mean change") in future time slices from the baseline period which is calculated using Eq. (2). Associated with the ensemble mean change is uncertainty, obtained using Eq. (1), which is represented by error bars in the figure. Uncertainty limits reflect the average deviation of change in the mean of individual GCMs from the ensemble mean.

T2 in case of RCP 4.5 emission scenario is observed to exhibit maximum change for all the three regions along with high uncertainties. High confidence level associated with T2 imply probable impacts in hydrologic response associated with this time slice. RCP 8.5 emission scenario, for most of the time slices, exhibits moderately significant change which may result in less probable impacts.

Upon assessing the monthly variability in P, it is observed that it may decline significantly during monsoon months whereas there might be an increase during winter months (October, November, December, January) across the three regions. This may result in shift in seasonal pattern of P in the region. Furthermore, if analyzed longitudinally from upstream to downstream it is noticed that the variation in P in downstream region is much more severe.

Annual mean T_{max} and T_{min}, are observed to show an increasing trend for future scenarios. Upon assessing the monthly variability, mean T_{max} and T_{min} are observed to increase significantly during winter months and they may decline during April to

HESSD
12, 2201–2242, 2015

September in all the regions. Results corresponding to ensemble change in mean annual T_{max} and T_{min} from the baseline are shown in Fig. 7, center and bottom panels respectively. Change in T_{max} and T_{min} can affect the hydrology by changing rain to snow ratio, ET and consequently runoff (Christensen et al., 2004). Therefore change in T may affect the overall water availability in the basin. On assessing the change in T longitudinally over UGB, it is observed that downstream region may experience maximum increase in the annual mean T_{max} and T_{min} thus causing serious implication in this part of the UGB. Downstream region, as mentioned earlier, may suffer from sporadic P along with significant increase in T, resulting in severe water availability problem in this part of the UGB. This condition may prove to be detrimental from agricultural point of view as this area is heavily under cultivation (86 % of total downstream area).

Upon evaluating the emission scenario based uncertainty, it is found that there is no significant difference between the two scenarios RCP 4.5 and RCP 8.5 which indicates that the scenario based uncertainty will be minimum. Impacts of changes in P and T on streamflow are presented in Sect. 3.3.2.

3.3 Hydrologic responses to land use and climate change

To evaluate the effects of land use (LU) and climate change on the hydrology of the study area, three scenarios are considered. The first two scenarios are based on the single factor approach (Li et al., 2009), i.e., one driving factor is changed at an instant keeping the other constant. In the first scenario, climate is considered invariant while LU is varied with time whereas in the second scenario, LU is considered invariant while climate is varied with time. These two scenarios are constructed to understand how streamflow would respond if only one of the driving forces is changed with time thereby assisting in quantifying the influence of individual factors on streamflow. In reality, both LU and climate change simultaneously with time and the hydrologic response is generated based on their integrated effect which is addressed by the third scenario. Finally from the integrated response, contributions of LU and climate on the streamflow variability is segregated using results from the other two scenarios. In depth analysis in the

HESSD
12, 2201–2242, 2015

CC BY

first two scenarios is carried out due to lack of detailed studies that examine the effects of LU and climate change on streamflow in the UGB.

3.3.1 Impact of land use change

In order to investigate hydrological impacts of LU change, simulations are carried out keeping climate fixed at 1971 while LU is changed progressively from 1971 to 2011. LU in any region changes gradually over a period of time and therefore starting and ending years may satisfactorily represent the change that has occurred in each LU class. Considering this, LU of the intermittent years can be obtained using rate of change in each LU class between the starting and ending years. It is to be noted that to obtain LU information for 1971 and 1972, rate of change between 1973 and 1980 is considered. LU obtained for each year is then used to drive the VIC model to obtain simulations under LU effect with invariant climate. Although simulations are carried out continuously from 1971 to 2011, for the sake of brevity, results corresponding to the starting year (1971) and the ending year (2011) for all the three regions are presented in Fig. 8.

It can be observed from the Fig. 8 that from 1971 to 2011, there is an increase in the magnitude of peak discharge for the upstream and midstream regions. This observation is consistent with other studies reported in literature which state that LU change has pronounced effect on peak flows (Tollan, 2002). No change in the discharge regime of the downstream region is noticed. LU and topography of the region is observed to have a conspicuous effect on the hydrologic response from the basin which is reflected in the hydrograph patterns for the three regions. Rising limb of the upstream region (Fig. 8a) begins during April while for midstream and downstream (Fig. 8b and c respectively) it occurs during May–June. The early occurrence of rising limb in upstream region can be attributed to the snowmelt runoff contribution to the streamflow. However, for midstream and downstream regions, rising limb begins with the onset of monsoon. The recession limb of hydrograph for upstream region falls quickly owing to the steep slope of the region. For midstream, a sharp drop is observed up to a certain level during October indicating the termination of direct runoff contribution to streamflow. Following

HESSD
12, 2201–2242, 2015

CC BY

this, the contribution is predominantly through baseflow which in this case is observed to be higher than the baseflow before the monsoon months. The higher baseflow during post monsoon period could be attributed to slow release of water stored by forests (dense and scrub) in the region aided by low elevation of the terrain in the region. Downstream region, though entirely a flat terrain, is dominated by crop land and urban areas that lack the capacity of holding the water, therefore limiting the contribution of baseflow to streamflow which leads to the observed sharp decline in recession limb. Furthermore, long term impacts of LU change are more evident in annual streamflow which is observed to increase by 12, 17 and 1 % from 1971 to 2011 for upstream, midstream and downstream regions respectively.

Sensitivity of the region to different LU categories is assessed in separate simulations. In this case, simulations considering each LU class are performed and change in streamflow under each category is quantified. To quantify the magnitude of change in streamflow caused by change in LU, ratio between streamflow and LU is computed. The ratio is referred to as Runoff-LU ratio (RL) in the present study. The RL indicates the effect of 1 % change in any LU category on streamflow and aids in identifying the significance of a particular LU class in determining the hydrologic response. Based on the ratios obtained, streamflow response (to a particular LU category) is classified under three categories: (i) highly sensitive if RL is ≥ 3. It indicates that a change of 1 % in LU category results in the change of hydrologic response by at least three times, (ii) moderately sensitive, ($1 \leq \mathrm{RL} \leq 2$); and (iii) insensitive, ($0 < \mathrm{RL} < 1$). Sign associated with the RL indicates the direction of impact

It can be observed from Table 4 that in the upstream region, RL is maximum for the urban area implying that the hydrologic response in this region is highly sensitive to the changes in urban area. It can be inferred that 1 % change in the urban area results in 4 % increase in the streamflow from the upstream region. The upstream region has significant portion of area under dense forest that has shown minor increase in the last decade (2000 to 2011) (Table 3). The simulated streamflow is observed to be moderately sensitive to this increase, though the observed impact is in the opposite direction,

CC BY

i.e., increase in forest results in decrease in streamflow. Furthermore, streamflow simulated from the upstream region is moderately sensitive to crop lands as well. Midstream region has crop land as the dominant LU type covering 53 % of the area during 1971 and 81 % of the area in 2011, streamflow is observed to be moderately sensitive to it. It is also observed that streamflow is moderately sensitive to urban area in this region. Though the downstream region is predominantly cultivated land (approximately 85 % of the area), hydrologic response is observed to be moderately sensitive to changes in the urban area. High sensitivity of streamflow from the regions to urban area can be attributed to the fact that increase in urban sprawl could reduce the infiltration resulting in generation of higher surface runoff. Thus all the three regions of the UGB are observed to be moderately sensitive to change in crop land area while moderately to highly sensitive to change in urban area.

3.3.2 Impact of climate change

In order to investigate the individual impact of changing climate on hydrology, simulations are carried out keeping LU fixed for 1971 and altering climate continuously for the baseline period (1971–2005) and future emission scenarios (2010–2100). The simulation results obtained are referred to as Q_{clim} hereafter. To quantify the change in streamflow, the VIC model is driven using the downscaled, bias-corrected six GCM outputs and the simulation results obtained are compared with the baseline simulation results. Change in ensemble mean annual Q_{clim} for five future time slices from the baseline annual streamflow for the three regions is presented in Fig. 9 with the associated uncertainties shown as error bars.

From the Fig. 9, it can be observed that change in Q_{clim} has patterns similar to that of change in mean annual P (Fig. 8, top panel). Change in Q_{clim} for all the time slices is observed to be moderate to highly significant in most of the cases indicating probable impacts of climate change on hydrologic response of the basin. Uncertainty is observed to increase through the time slices and maximum uncertainty in projection results for all the three regions is observed in T5. Although the two scenarios gave consistent

HESSD
12, 2201–2242, 2015

CC BY

results, to address the issue of scenario based uncertainty, mean of ensemble annual Q_{clim} series of RCP 4.5 is compared with mean of ensemble annual Q_{clim} series of RCP 8.5. The two means are found to be moderately different for the midstream region, indicating the need to consider the two scenarios as separate cases.

Assessment of the monthly variations in the Q_{clim} across future time slices indicated that Q_{clim} may decrease for JAS months for the three regions while it may increase during the months of October, November and December (OND). The variations observed in Q_{clim} during JAS and OND are found to be consistent with that of P. However, this is not true for all the months such as June, where P is observed to decrease in future while Q_{clim} is observed to increase which can be attributed to decrease in T that may reduce evaporation from the region resulting in higher runoff. Similar kind of response of streamflow to P and T in a catchment is reported in literature for a different case study by Fu et al. (2007). To further assess the sensitivity of Q_{clim} to changes in P and T and quantify their effect, runoff ratio (RR) is computed using average annual runoff and rainfall for each time slice. Results pertaining to the values of RR are presented in Table 5.

RR is a simple index that reflects the relationship between P and Q_{clim} by determining the proportion of P that gets converted to Q_{clim} (Zhang et al., 2011). RR is calculated by normalizing the Q_{clim} with P within the same time scale. Analyzing RR over a period of time on the same river basin (under same LU conditions) aids in understanding topographic response and effect of climate on streamflow. In the present study, longitudinal variation in RR strikingly depicts the watershed topography from upstream to downstream. RR is observed to be 60 % for the upstream region, 44 % for the midstream region and 23 % for the downstream region during the baseline period. Upstream region is characterized by mountainous terrain and steep slopes thus most of the P gets converted to Q_{clim} (high RR), whereas downstream region has very flat terrain thus much of the P get evaporated or infiltrated into soil and little gets converted to Q_{clim} (low RR). Analysis of RR over the different time slices for a particular region indicate that in general, when P does not change significantly from the baseline period,

HESSD
12, 2201–2242, 2015

increase in T results in reduced RR. This is intuitive as increase in T leads to loss of water as evaporation which reduces Q_{clim} and consequently lessens RR. The RR is observed to increase and approach towards baseline RR with slight increase in P (irrespective of change in T). In such cases, temperature variations are seen to be of less importance. In most of the cases it is observed that decrease in P results in decrease in RR, but in few cases such as T4 and T5 (RCP 4.5 and RCP 8.5) for downstream region, P is observed to reduce accompanied by an increase in T. In such a case, one might expect RR to reduce significantly which is not observed. This anomaly could be attributed to occurrence of short duration dense rainfall events in the region. Reduction in RR is observed in case when P is observed to increase with no significant change in T. This kind of behavior could be due to shift in seasonal pattern of P or due to increased inter-arrival time between the two P events. In summary, Q_{clim} from the downstream region is observed to be very sensitive to the changes in P whereas Q_{clim} is sensitive to P up to a certain threshold for midstream region, beyond which T_{max} also starts playing a role. Owing to the complex topography and climatology of the upstream region, it is difficult to interpret the sensitivity of Q_{clim} to different climate factors.

3.3.3 Integrated impacts of land use and climate change

In a real world situation, change in LU and climate occurs simultaneously and the impact of both these factors is reflected in the streamflow. To carry out analysis pertaining to this scenario, one needs concurrent information on LU and climate. Under this notion, VIC model is driven for 1971–2005 (baseline period) across the three region in the UGB. It is to be noted that the process of obtaining projections of future LU conditions in the basin does not come under the purview of present work. Therefore, integrated impact of LU and climate change on future streamflow could not be assessed. The results obtained from this analysis can be interpreted as the streamflow simulations under simultaneous change in LU and climate conditions (hereafter referred to as Q_{int}). In order to assess decadal variations in streamflow of the UGB, baseline period is aggregated to four time periods: P1 (1971–1980); P2 (1981–1990); P3 (1991–2000) and

HESSD
12, 2201–2242, 2015

CC BY

P4 (2001–2005), although, VIC model is executed for the entire duration. Results corresponding to Q_{int} for upstream, midstream and downstream regions are presented in Table 6. It is observed that no clear inference about the implication of LU and climate on streamflow can be achieved from the obtained Q_{int} values due to large variability in the streamflow corresponding to the variability in rainfall. Therefore a further analysis is necessary to isolate the impacts of LU and climate on streamflow response which is presented in the following sub-section.

3.3.4 Isolating the impacts of land use and climate

In order to segregate the impacts of LU and climate, the proposed approach primarily requires results of Q_{int} (obtained from the Sect. 3.3.3), and Q_{clim} (obtained from the Sect. 3.3.2) over the same time period. Herein Q_{int} and Q_{clim} are comparable based on the fact that the respective simulations are obtained under identical conditions of hydrologic model and climatology. This condition reflects that the only changing subject among the two scenarios is the land use input to the hydrologic model. Therefore, the residue of the two scenarios, $Q_{int} - Q_{clim}$, is considered to be the exclusive contribution of LU to streamflow (hereafter referred to as Q_{LU}).

In the present case study, simulations of Q_{int} and Q_{clim} are obtained for the time periods P1, P2, P3 and P4 mentioned earlier for upstream, midstream and downstream regions. Q_{int} and Q_{clim} are then used to estimate Q_{LU}. Alongside, the percentage contributions of LU and climate to Q_{int} are also computed ($Q_{clim/LU}$ (%) $= \frac{Q_{clim/LU}}{Q_{int}} \times 100$). Table 6 presents results pertaining to these.

Results from Table 6 suggest that climate is the dominant contributor to streamflow across all the regions. Contribution of LU, on the other hand, is observed to be minimal. Further insight to the influence of LU to streamflow is obtained from the inferences drawn from Sect. 3.3.1. It is observed from the analysis is Sect. 3.3.1 that streamflow is highly sensitive to changes in urban land in upstream and downstream regions while it is moderately sensitive to urban and crop land areas in midstream region. The spatial

CC BY

extent of urban area is observed to be very less in the upstream and downstream regions (less than 10 %), which could have resulted in negligible contribution of LU to streamflow. For the midstream region, despite ∼ 70 % of the area is under crop land, contribution of LU to streamflow turned out to be less. This could be due to moderate sensitivity of streamflow to the changes in crop land category. It is well understood that crop lands contribute more to the ET than to the streamflow. Contribution of urban area to streamflow is negligible due to its less spatial extent in the midstream region. When Q_{LU} (%) is assessed across the time periods in the three regions, it is observed that there is gradual increase in the contribution of LU to streamflow. This could be attributed to the fact that area under the sensitive LU categories (urban area and crop land) is increasing with time in the regions.

In the present study, the application of proposed methodology of isolating the hydrologic impacts of LU and climate is limited only to the baseline period due to unavailability of future LU information. However, this approach can be applied to the future time periods as well upon obtaining future LU projections along with climate simulations. This is illustrated by conducting the analysis on T1 (2010–2020) wherein Q_{int} is obtained by driving VIC model under LU condition of 2011 (assuming that LU may not change significantly during this decade) and climate simulations from six GCMs for the corresponding time period. Results for the T1 are presented in Table 7.

From Table 7, it can be observed that the contribution of LU to streamflow from upstream region has increased (compared to P4). This could be attributed to increase in area under urban land by 65 % in T1 from P4 in the upstream region. No significant increase is observed in crop land and urban land areas in T1 from P4 for midstream and downstream regions respectively (2 % increase in crop land in midstream region and 20 % increase in urban area in downstream region) which could have resulted in unvarying contribution of LU to streamflow from P4 (Table 6) to T1 (Table 7) in these regions.

From the analysis, it can be concluded that the proposed approach can be applied over a watershed with a well calibrated and validated hydrologic model. Future work

HESSD
12, 2201–2242, 2015

CC BY

involves generating LU projections for future time periods which can be corroborated with climate projections described in Sect. 3.3.2 to isolate the impacts of LU and climate on future streamflow simulations.

4 Conclusions

In the present paper a hydrologic modelling based methodology is presented to isolate the impacts of LU and climate on streamflow in a river basin. To achieve this, three scenarios are considered that assess the individual and integrated impacts of LU and climate on streamflow. In-depth assessment of impact of LU and climate change on streamflow of the UGB is conducted as part of this study. The analysis is carried out by applying a calibrated and validated VIC model over the upstream, midstream and downstream regions of the UGB. The LU change analysis indicated that the areas of crop land and urban land have increased manifold since 1970s. Streamflow is observed to be moderately to highly sensitive to the change in urban area. From the climate change analysis, it is observed that rainfall (P) may decrease during the monsoon months and increase during the winter months which may result in shift in seasonal P pattern. Annual means of T_{max} and T_{min} are also observed to increase in the future. Streamflow is observed to reproduce the variations in P. All the changes in P, T_{max} and T_{min} pertaining to climate change scenario are found to be statistically significant from the baseline period, indicating that deviation in their magnitudes is likely to cause impacts on the hydrologic response.

The integrated effect of LU and climate change on streamflow is observed to be more prominent in the study area. Upon isolating the impact of LU and climate on streamflow it is observed that climate contributes more to the simulated streamflow (> 90 %). In contrast, LU did not contribute significantly to the simulated streamflow which could be attributed to less spatial extent of sensitive LU categories in the region.

The proposed approach is found to be generic, simple and applicable to any river basin to isolate the relative impacts of LU and climate change on streamflow. The case

HESSD
12, 2201–2242, 2015

CC BY

study analysis indicates that the change in climate may become a major concern in the UGB for water resources management.

Acknowledgement. The work is carried out as part of the MoES-NERC Changing Water Cycle (South Asia) project: hydro-meteorological feedbacks and changes in water storage and fluxes in Northern India (grant number: MoES/NERC/16/02/10 PC-II). Authors acknowledge the support of Indian Meteorological Department (IMD) and Indian Institute of Tropical Meteorology (IITM) for providing the data.

References

Arnell, N. W.: Uncertainty in the relationship between climate forcing and hydrological response in UK catchments, Hydrol. Earth Syst. Sci., 15, 897–912, doi:10.5194/hess-15-897-2011, 2011.

Beyene, T., Lettenmaier, D. P., and Kabat, P.: Hydrologic impacts of climate change on the Nile River Basin: implications of the 2007 IPCC scenarios, Climatic Change, 100, 433–461, doi:10.1007/s10584-009-9693-0, 2010.

Christensen, N. S. and Lettenmaier, D. P.: A multimodel ensemble approach to assessment of climate change impacts on the hydrology and water resources of the Colorado River Basin, Hydrol. Earth Syst. Sci., 11, 1417–1434, doi:10.5194/hess-11-1417-2007, 2007.

Christensen, N. S., Wood, A. W., Voisin, N., Lettenmaier, D. P., and Palmer, R. N.: The effects of climate change on the hydrology and water resources of the Colorado River basin, Climatic Change, 62, 337–363, doi:10.1023/B:CLIM.0000013684.13621.1f, 2004.

Cuo, L., Zhang, Y., Gao, Y., Hao, Z., and Cairang, L.: The impacts of climate change and land cover/use transition on the hydrology in the upper Yellow River Basin, China, J. Hydrol., 502, 37–52, doi:10.1016/j.jhydrol.2013.08.003, 2013.

Ekström, M., Jones, P. D., Fowler, H. J., Lenderink, G., Buishand, T. A., and Conway, D.: Regional climate model data used within the SWURVE project – 1: projected changes in seasonal patterns and estimation of PET, Hydrol. Earth Syst. Sci., 11, 1069–1083, doi:10.5194/hess-11-1069-2007, 2007.

Fu, G., Charles, S. P., and Chiew, F. H. S.: A two-parameter climate elasticity of streamflow index to assess climate change effects on annual streamflow, Water Resour. Res., 43, W11419, doi:10.1029/2007wr005890, 2007.

Ghosh, S. and Mujumdar, P. P.: Climate change impact assessment: uncertainty modeling with imprecise probability, J. Geophys. Res.-Atmos., 114, D18113, doi:10.1029/2008jd011648, 2009.

Giorgi, F. and Mearns, L. O.: Calculation of average, uncertainty range, and reliability of regional climate changes from AOGCM simulations via the "reliability ensemble averaging" (REA) method, J. Climate, 15, 1141–1158, doi:10.1175/1520-0442(2002)015<1141:coaura>2.0.co;2, 2002.

Hamlet, A. F. and Lettenmaier, D. P.: Effects of climate change on hydrology and water resources in the Columbia River basin, J. Am. Water Resour. As., 35, 1597–1623, doi:10.1111/j.1752-1688.1999.tb04240.x, 1999.

Islam, S. A., Bari, M. A., and Anwar, A. H. M. F.: Hydrologic impact of climate change on Murray–Hotham catchment of Western Australia: a projection of rainfall–runoff for future water resources planning, Hydrol. Earth Syst. Sci., 18, 3591–3614, doi:10.5194/hess-18-3591-2014, 2014.

Kendall, M. G.: A new measure of rank correlation, Biometrika, 30, 81–93, 1938.

Li, Z., Liu, W.-Z., Zhang, X.-C., and Zheng, F.-L.: Impacts of land use change and climate variability on hydrology in an agricultural catchment on the Loess Plateau of China, J. Hydrol., 377, 35–42, doi:10.1016/j.jhydrol.2009.08.007, 2009.

Liang, X., Lettenmaier, D. P., Wood, E. F., and Burges, S. J.: A simple hydrologically based model of land-surface water and energy fluxes for general-circulation models, J. Geophys. Res.-Atmos., 99, 14415–14428, doi:10.1029/94jd00483, 1994.

Lohmann, D., Raschke, E., Nijssen, B., and Lettenmaier, D. P.: Regional scale hydrology: I. Formulation of the VIC-2L model coupled to a routing model, Hydrolog. Sci. J., 43, 131–141, doi:10.1080/02626669809492107, 1998.

Mango, L. M., Melesse, A. M., McClain, M. E., Gann, D., and Setegn, S. G.: Land use and climate change impacts on the hydrology of the upper Mara River Basin, Kenya: results of a modeling study to support better resource management, Hydrol. Earth Syst. Sci., 15, 2245–2258, doi:10.5194/hess-15-2245-2011, 2011.

Mann, H. B.: Nonparametric tests against trend, Econometrica, 13, 245–259, doi:10.2307/1907187, 1945.

Maurer, E. P.: Uncertainty in hydrologic impacts of climate change in the Sierra Nevada, California, under two emissions scenarios, Climatic Change, 82, 309–325, doi:10.1007/s10584-006-9180-9, 2007.

CC BY

Maurer, E. P. and Hidalgo, H. G.: Utility of daily vs. monthly large-scale climate data: an intercomparison of two statistical downscaling methods, Hydrol. Earth Syst. Sci., 12, 551–563, doi:10.5194/hess-12-551-2008, 2008.
Nijssen, B., O'Donnell, G. M., Hamlet, A. F., and Lettenmaier, D. P.: Hydrologic sensitivity of global rivers to climate change, Climatic Change, 50, 143–175, doi:10.1023/a:1010616428763, 2001.
Oki, T. and Kanae, S.: Global hydrological cycles and world water resources, Science, 313, 1068–1072, doi:10.1126/science.1128845, 2006.
Ott, B. and Uhlenbrook, S.: Quantifying the impact of land-use changes at the event and seasonal time scale using a process-oriented catchment model, Hydrol. Earth Syst. Sci., 8, 62–78, doi:10.5194/hess-8-62-2004, 2004.
Rajeevan, M., Bhate, J., Kale, J. A., and Lal, B.: High resolution daily gridded rainfall data for the Indian region: analysis of break and active monsoon spells, Curr. Sci. India, 91, 296–306, 2006.
Refsgaard, J. C. and Knudsen, J.: Operational validation and intercomparison of different types of hydrological models, Water Resour. Res., 32, 2189–2202, doi:10.1029/96wr00896, 1996.
Renner, M., Seppelt, R., and Bernhofer, C.: Evaluation of water-energy balance frameworks to predict the sensitivity of streamflow to climate change, Hydrol. Earth Syst. Sci., 16, 1419–1433, doi:10.5194/hess-16-1419-2012, 2012.
Renner, M., Brust, K., Schwärzel, K., Volk, M., and Bernhofer, C.: Separating the effects of changes in land cover and climate: a hydro-meteorological analysis of the past 60 yr in Saxony, Germany, Hydrol. Earth Syst. Sci., 18, 389–405, doi:10.5194/hess-18-389-2014, 2014.
Rientjes, T. H. M., Haile, A. T., Kebede, E., Mannaerts, C. M. M., Habib, E., and Steenhuis, T. S.: Changes in land cover, rainfall and stream flow in Upper Gilgel Abbay catchment, Blue Nile basin – Ethiopia, Hydrol. Earth Syst. Sci., 15, 1979–1989, doi:10.5194/hess-15-1979-2011, 2011.
Rose, S. and Peters, N. E.: Effects of urbanization on streamflow in the Atlanta area (Georgia, USA): a comparative hydrological approach, Hydrol. Process., 15, 1441–1457, doi:10.1002/hyp.218, 2001.
Scanlon, B. R., Jolly, I., Sophocleous, M., and Zhang, L.: Global impacts of conversions from natural to agricultural ecosystems on water resources: quantity versus quality, Water Resour. Res., 43, W03437, doi:10.1029/2006wr005486, 2007.

HESSD
12, 2201–2242, 2015

CC BY

Singh, D., Horton, D. E., Tsiang, M., Haugen, M., Ashfaq, M., Mei, R., Rastogi, D., Johnson, N. C., Charland, A., Rajaratnam, B., and Diffenbaugh, N. S.: Severe precipitation in northern india in june 2013: causes, historical context, and changes in probability, B. Am. Meteorol. Soc., 95, S58–S61, 2014.

Tollan, A.: Land-use change and floods: what do we need most, research or management?, Water Sci. Technol., 45, 183–190, 2002.

Vorosmarty, C. J., Green, P., Salisbury, J., and Lammers, R. B.: Global water resources: vulnerability from climate change and population growth, Science, 289, 284–288, doi:10.1126/science.289.5477.284, 2000.

Wada, Y., van Beek, L. P. H., and Bierkens, M. F. P.: Modelling global water stress of the recent past: on the relative importance of trends in water demand and climate variability, Hydrol. Earth Syst. Sci., 15, 3785–3808, doi:10.5194/hess-15-3785-2011, 2011.

Wagner, P. D., Kumar, S., and Schneider, K.: An assessment of land use change impacts on the water resources of the Mula and Mutha Rivers catchment upstream of Pune, India, Hydrol. Earth Syst. Sci., 17, 2233–2246, doi:10.5194/hess-17-2233-2013, 2013.

Wang, G. Q., Zhang, J. Y., Jin, J. L., Pagano, T. C., Calow, R., Bao, Z. X., Liu, C. S., Liu, Y. L., and Yan, X. L.: Assessing water resources in China using PRECIS projections and a VIC model, Hydrol. Earth Syst. Sci., 16, 231–240, doi:10.5194/hess-16-231-2012, 2012.

Wang, S., Kang, S., Zhang, L., and Li, F.: Modelling hydrological response to different land-use and climate change scenarios in the Zamu River basin of northwest China, Hydrol. Process., 22, 2502–2510, doi:10.1002/hyp.6846, 2008.

Wang, S., Zhang, Z., McVicar, T. R., Guo, J., Tang, Y., and Yao, A.: Isolating the impacts of climate change and land use change on decadal streamflow variation: assessing three complementary approaches, J. Hydrol., 507, 63–74, doi:10.1016/j.jhydrol.2013.10.018, 2013.

Wood, A. W., Maurer, E. P., Kumar, A., and Lettenmaier, D. P.: Long-range experimental hydrologic forecasting for the eastern United States, J. Geophys. Res.-Atmos., 107, ACL 6-1–ACL 6-15, doi:10.1029/2001jd000659, 2002.

Zhang, Y., Guan, D., Jin, C., Wang, A., Wu, J., and Yuan, F.: Analysis of impacts of climate variability and human activity on streamflow for a river basin in northeast China, J. Hydrol., 410, 239–247, 2011.

HESSD

12, 2201–2242, 2015

CC BY

HESSD
12, 2201–2242, 2015

Table 1. GCMs from the CORDEX project used in the present study.

Modeling Center-Experiment Name	Driving GCM (Abbreviation)	Institution
Commonwealth Scientific and Industrial Research Organization, (CSIRO) Australia – CCAM	ACCESS1.0 (ACC)	CSIRO
	CNRM-CM5 (CNR)	Centre National de Recherches Meteorologiques
	CCSM4 (CCS)	National Center for Atmospheric Research
	GFDL-CM3 (GFD)	Geophysical Fluid Dynamics Laboratory
	MPI-ESM-LR (MPI)	Max Planck Institute for Meteorology (MPI-M)
	NorESM1-M (NOR)	Norwegian Climate Centre

CC BY

Table 2. Structure of VIC model obtained for the upstream and midstream region along with the performance measures during calibration and validation phase.

Region	No. of candidate models	Value of optimum set of parameters	Calibration				Validation			
			R^2	E_{NRMSE}	E_{NSE}	β	R^2	E_{NRMSE}	E_{NSE}	β
Upstream	47	$B = 0.13$; Ds = 0.0005; Ws = 0.76	0.77	0.23	0.77	−0.02	0.83	0.29	0.79	−0.18
Midstream	80	$B = 0.044$; Ds = 0.0004; Ws = 0.62	0.88	0.14	0.86	0.12	0.71	0.47	0.53	−0.04

HESSD
12, 2201–2242, 2015

Isolating the impacts of land use and climate change on streamflow

I. Chawla and P. P. Mujumdar

CC BY

Table 3. LU analysis of UGB for years 1973, 1980, 2000 and 2011.

Category	Area (km^2)				% Change
	1973	1980	2000	2011	between 1973–2011
Snow	9071	9933	6210	5241	−42.23
Dense Forest	13 843	12 172	10 913	14 146	2.19
Scrub Forest	22 534	14 061	13 238	8579	−61.93
Crop Land	43 048	50 661	61 380	63 127	46.64
Barren Land	4795	6135	587	179	−96.26
Urban Area	1384	1493	2173	3078	122.39
Water	714	847	982	1069	49.72
Total	95 390	95 302	95 484	95 419	

HESSD
12, 2201–2242, 2015

I. Chawla and P. P. Mujumdar

CC BY

Table 4. Runoff-LU ratio for different LU categories for upstream, midstream and downstream regions.

Region	LU classes			
	Crop	Urban	Forest	Barren
Upstream	2.05	4.02	−1.31	0.91
Midstream	1.49	1.17	0.1	0.97
Downstream	0.63	2.69	0.9	0.93

HESSD
12, 2201–2242, 2015

Isolating the impacts of land use and climate change on streamflow

I. Chawla and P. P. Mujumdar

Table 5. Runoff Ratio across time slices for upstream, midstream and downstream regions (terms in parentheses indicate the percent change from the baseline values).

Region	Time Period	Rainfall (mm) RCP 4.5	Rainfall (mm) RCP 8.5	Runoff (mm) RCP 4.5	Runoff (mm) RCP 8.5	Runoff Ratio RCP 4.5	Runoff Ratio RCP 8.5
Upstream	Baseline	1294	1294	772	772	0.60	0.60
	T1	1196 ± 172 (−8)	1210 ± 46(−7)	697 ± 84 (−10)	683 ± 32(−12)	0.58 (−2)	0.56 (−4)
	T2	1084 ± 480(−16)	1257 ± 43(−3)	619 ± 287(−20)	715 ± 30 (−7)	0.57 (−3)	0.57 (−3)
	T3	1377 ± 171 (+6)	1323 ± 32(+2)	816 ± 137 (+6)	771 ± 26 (0)	0.59 (−1)	0.58 (−2)
	T4	1416 ± 198 (+9)	1357 ± 42(+5)	845 ± 163 (+9)	800 ± 38 (+4)	0.60 (0)	0.59 (−1)
	T5	1424 ± 182(+10)	1405 ± 27(+9)	854 ± 148(+11)	842 ± 26 (+9)	0.60 (0)	0.60 (0)
Midstream	Baseline	1009	1009	441	441	0.44	0.44
	T1	844 ± 84 (−16)	871 ± 63(−14)	323 ± 31 (−27)	328 ± 56(−25)	0.38 (−12)	0.38 (−4)
	T2	787 ± 265 (−22)	884 ± 53(−12)	296 ± 115(−33)	332 ± 52(−25)	0.38 (−12)	0.38 (−12)
	T3	1003 ± 135 (−1)	952 ± 31 (−6)	413 ± 77 (−6)	378 ± 20(−14)	0.41 (−3)	0.40 (−4)
	T4	1062 ± 159 (+5)	1016 ± 28(+1)	462 ± 101 (+5)	427 ± 23 (−3)	0.44 (0)	0.42 (−2)
	T5	1071 ± 160 (+6)	1058 ± 21(+5)	471 ± 121 (+7)	452 ± 21 (+3)	0.44 (0)	0.43 (−1)
Downstream	Baseline	826	826	192	192	0.23	0.23
	T1	579 ± 63 (−30)	590 ± 55(−29)	102 ± 13 (−47)	107 ± 19(−44)	0.18 (−5)	0.18 (−5)
	T2	557 ± 183 (−32)	589 ± 40(−29)	89 ± 43 (−54)	104 ± 13(−46)	0.16 (−7)	0.18 (−5)
	T3	721 ± 108 (−13)	663 ± 38(−20)	141 ± 34 (−27)	127 ± 13(−34)	0.20 (−3)	0.19 (−4)
	T4	743 ± 128 (−10)	731 ± 23(−11)	150 ± 46 (−22)	148 ± 7 (−23)	0.20 (−3)	0.20 (−3)
	T5	785 ± 101 (−5)	771 ± 37 (−6)	173 ± 36 (−10)	167 ± 16(−13)	0.22 (−1)	0.21 (−2)

HESSD
12, 2201–2242, 2015

CC BY

Table 6. Contribution of climate and LU to the streamflow for different time periods.

Region	Streamflow	P1 (1971–1980)	P2 (1981–1990)	P3 (1991–2000)	P4 (2001–2005)
Upstream	Q_{int} ($m^3 s^{-1}$)	775	772	859	823
	Q_{clim} ($m^3 s^{-1}$)	760	741	824	777
	Q_{clim} (%)	98	96	96	94
	Q_{LU} ($m^3 s^{-1}$)	15	31	35	46
	Q_{LU} (%)	2	4	4	6
Midstream	Q_{int} ($m^3 s^{-1}$)	1130	1183	1266	1195
	Q_{clim} ($m^3 s^{-1}$)	1108	1110	1182	1107
	Q_{clim} (%)	98	94	93	93
	Q_{LU} ($m^3 s^{-1}$)	22	73	84	88
	Q_{LU} (%)	2	6	7	7
Downstream	Q_{int} ($m^3 s^{-1}$)	123	103	85	78
	Q_{clim} ($m^3 s^{-1}$)	122	103	85	77
	Q_{clim} (%)	100	100	99	98
	Q_{LU} ($m^3 s^{-1}$)	1	0	1	1
	Q_{LU} (%)	0	0	1	2

HESSD
12, 2201–2242, 2015

Table 7. Contribution of LU and climate to streamflow during T1 (2010–2020) time slice under RCP 4.5 and RCP 8.5 emission scenarios.

Streamflow	Upstream		Midstream		Downstream	
	RCP 4.5	RCP8.5	RCP 4.5	RCP8.5	RCP 4.5	RCP8.5
Q_{int} ($m^3 s^{-1}$)	800 ± 72	789 ± 28	1008 ± 110	971 ± 138	52 ± 5	56 ± 11
Q_{clim} ($m^3 s^{-1}$)	713 ± 62	703 ± 23	938 ± 132	903 ± 123	51 ± 5	55 ± 11
Q_{clim} (%)	89	89	93	93	98	98
Q_{LU} ($m^3 s^{-1}$)	87 ± 10	86 ± 5	70 ± 23	68 ± 16	1 ± 0	1 ± 0
Q_{LU} (%)	11	11	7	7	2	2

HESSD
12, 2201–2242, 2015

CC BY

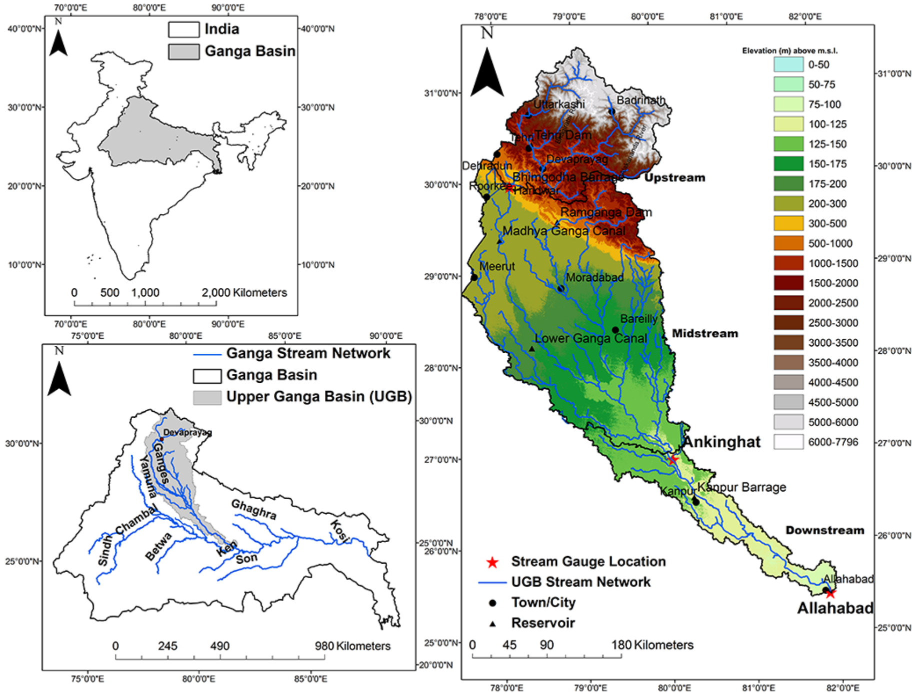

Figure 1. Location map and details of the UGB.

CC BY

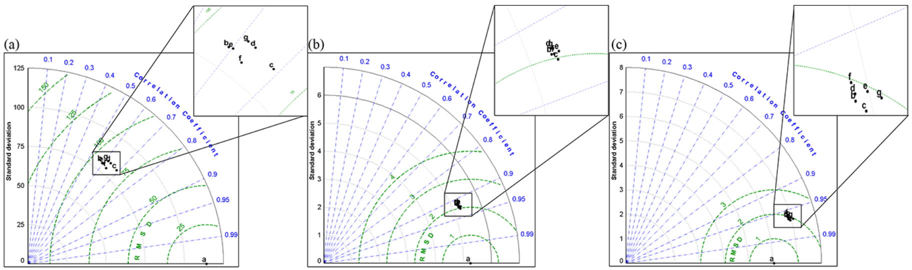

Figure 2. Taylor diagram for **(a)** Rainfall (mm) **(b)** T_{max} (°C) and **(c)** T_{min} (°C) for upstream region.

HESSD
12, 2201–2242, 2015

Isolating the impacts of land use and climate change on streamflow

I. Chawla and P. P. Mujumdar

CC BY

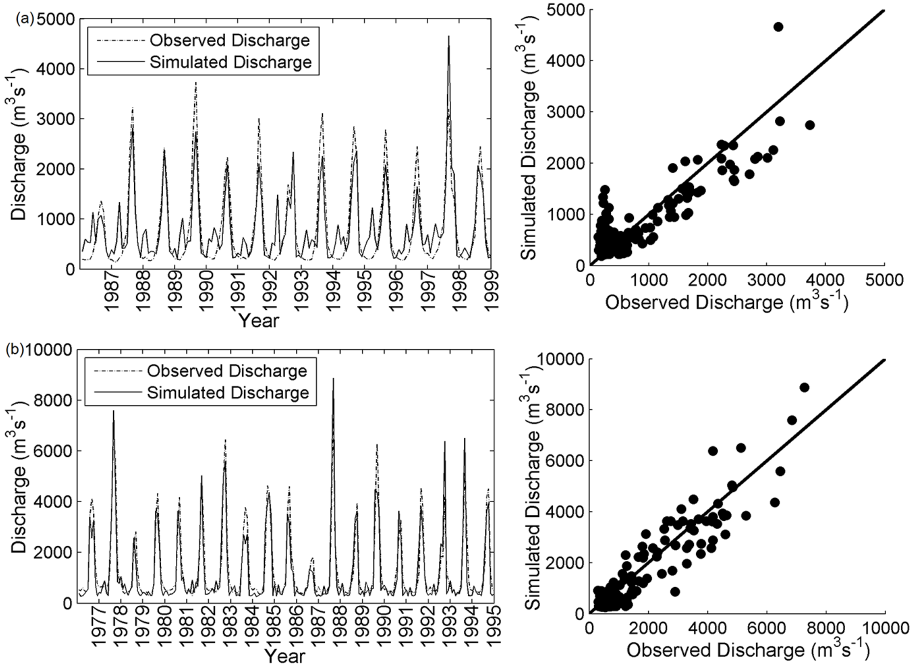

Figure 3. Calibration results of **(a)** upstream and **(b)** midstream region.

HESSD
12, 2201–2242, 2015

Isolating the impacts of land use and climate change on streamflow

I. Chawla and P. P. Mujumdar

Title Page
Abstract Introduction
Conclusions References
Tables Figures
◂ ▸
Back Close
Full Screen / Esc
Printer-friendly Version
Interactive Discussion

CC BY

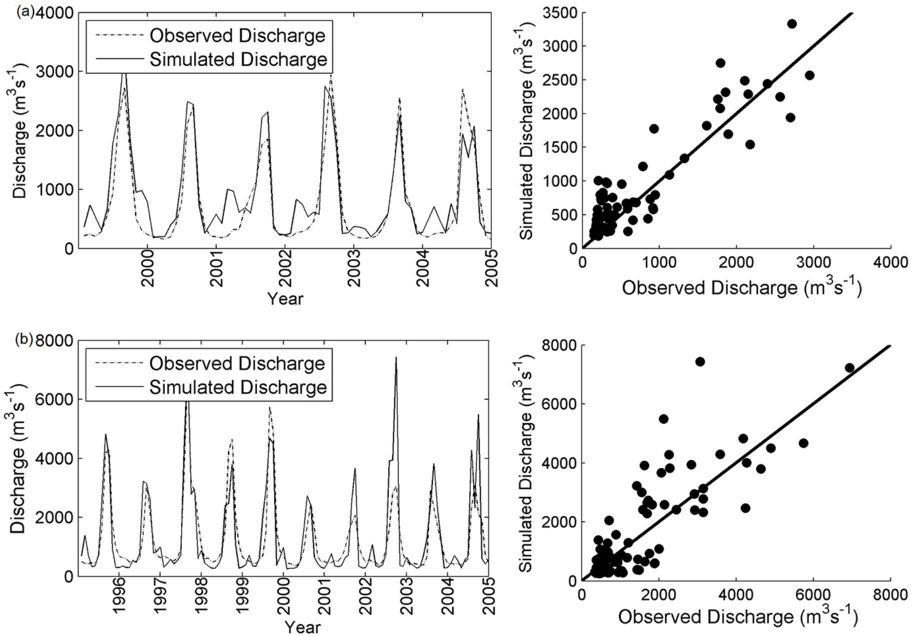

Figure 4. Validation results of **(a)** upstream and **(b)** midstream region.

CC BY

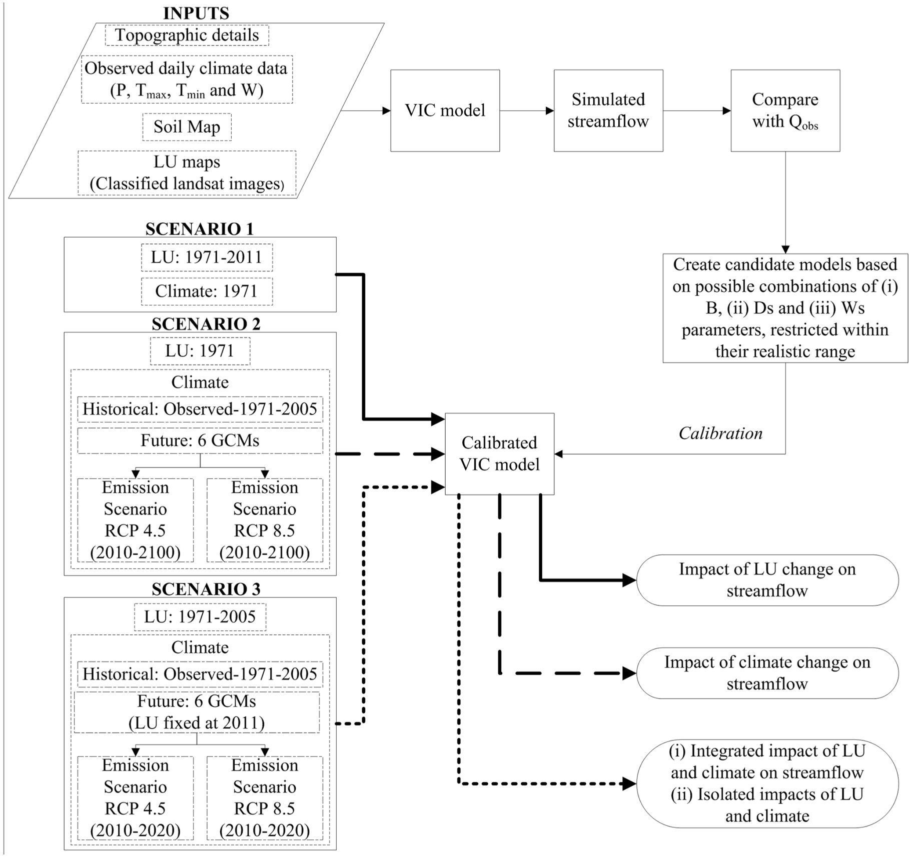

Figure 5. Overview of the work.

HESSD
12, 2201–2242, 2015

CC BY

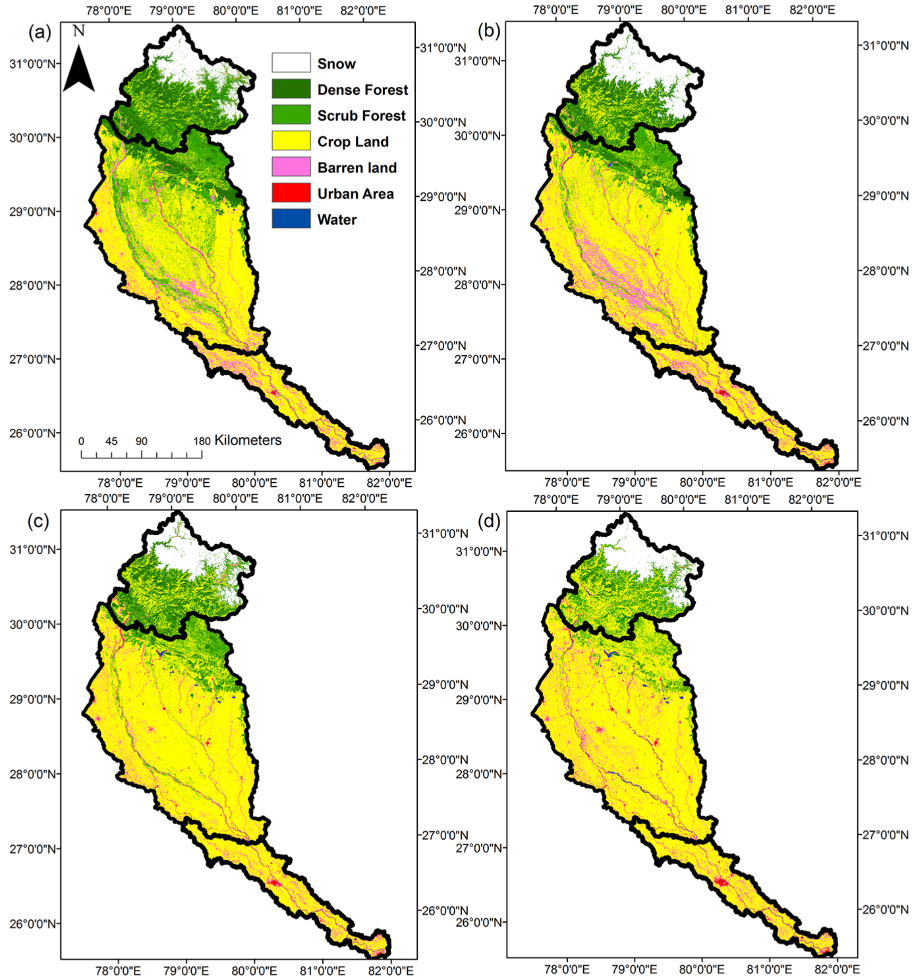

Figure 6. LU maps for **(a)** 1973, **(b)** 1980, **(c)** 2000 and **(d)** 2011.

HESSD
12, 2201–2242, 2015

CC BY

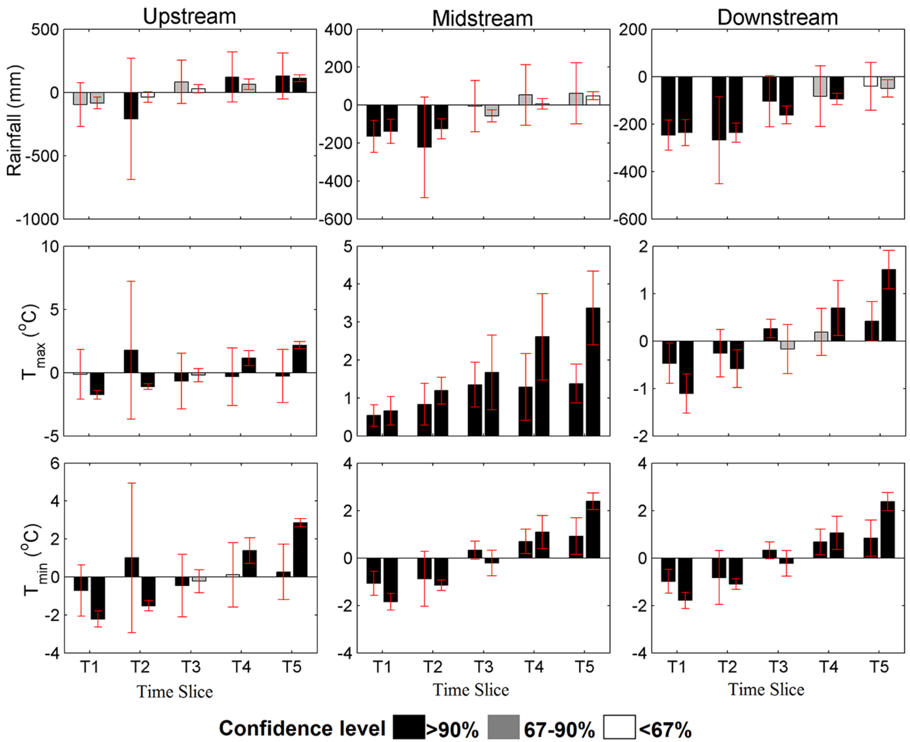

Figure 7. Change in the ensemble mean of rainfall (top panel), T_{max} (center panel) and T_{min} (bottom panel) from the baseline period for RCP 4.5 (first bar of a time slice) and RCP 8.5 scenarios (second bar of a time slice) at each time slice (T1: 2010–2020; T2: 2021–2040; T3: 2041–2060; T4: 2061–2080 and T5: 2081–2100).

HESSD
12, 2201–2242, 2015

I. Chawla and P. P. Mujumdar

CC BY

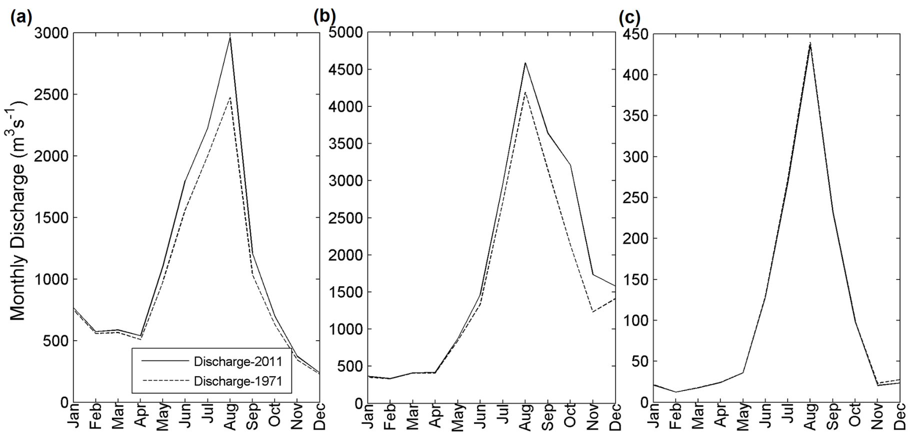

Figure 8. Simulation results for year 1971 and 2011 for **(a)** upstream, **(b)** midstream and **(c)** downstream region.

CC BY

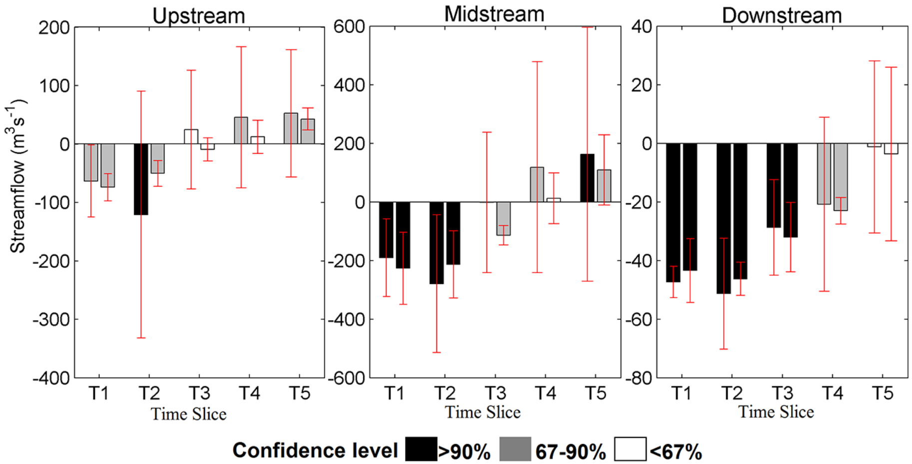

Figure 9. Change in ensemble mean of Q_{clim} from the baseline period for RCR 4.5 (first bar of every time slice of all the plots) and RCP 8.5 (second bar of every time slice of all the plots) scenarios at each time slice (T1: 2010–2020; T2: 2021–2040; T3: 2041–2060; T4: 2061–2080 and T5: 2081–2100).

CC BY